

# Multiparticle Aspects of $e^+e^-$ Interactions at an Energy of 133 GeV at LEP

Claus Grupen

Department of Physics, University of Siegen

D-57068 Siegen, Germany

e-mail: claus.grupen@cern.ch

## ABSTRACT

Multiparticle aspects in  $e^+e^-$  collisions at center-of-mass energies beyond the Z mass are investigated. To this end, data taken at 130 and 136 GeV with the four LEP detectors ALEPH, DELPHI, L3 and OPAL with an integrated luminosity of about  $5 \text{ pb}^{-1}$  per experiment are analyzed. A large number of events originate from radiative returns to the Z, i.e.  $e^+e^- \rightarrow Z \rightarrow e^+e^-$  with well understood Z-decays. The interesting events with a visible energy corresponding to the c.m.s. energy show features as expected from the extrapolation from the Z. One experiment (ALEPH) finds in four-jet final states some evidence for a clustering of the sum of di-jet masses around 105 GeV, which however, is not supported by the three other LEP collaborations. A preliminary analysis of data taken at a center-of-mass energy of  $\sqrt{s} = 161 \text{ GeV}$  shows agreement with QCD expectations.

## 1. Introduction

The large electron-positron collider (LEP) at CERN was upgraded in November 1995 from a center-of-mass energy of  $\sqrt{s} = 91 \text{ GeV}$  (on the Z peak) to  $\sqrt{s} = 130 - 140 \text{ GeV}$ . The total number of events collected per experiment was about 1500 corresponding to an integrated luminosity of  $5.5 \text{ pb}^{-1}$ . The bulk of data was taken at 130 GeV and 136 GeV in about equal proportion. Only  $0.04 \text{ pb}^{-1}$  was obtained at 140 GeV.

The running at an intermediate energy between LEP I (on the Z-peak) and LEP II ( $\sqrt{s} = 2 M_W$ ) has been named LEP 1.5. LEP 1.5 can check the running of  $\alpha_s$ , the coupling constant of strong interactions. Also, the measurement of infrared sensitive quantities like jet rates and event shape distributions allows a comparison with perturbative QCD calculations. Infrared sensitive quantities like multiplicities and inclusive particle production cannot be calculated perturbatively, but the experimental results can be compared to the energy evolution, which is predicted by quantum chromodynamics (QCD). Possible deviations would hint at deficiencies of particular Monte Carlo models or the presence of unexpected physical processes.

A drawback of LEP 1.5 is that the event rates are much lower compared to running on the Z-peak. On the other hand the effects of hadronization, which cannot be calculated in QCD, are predicted to be smaller at high  $\sqrt{s}$ . Therefore perturbative

Invited talk given at the "XXVI International Symposium on Multiparticle Dynamics" held in Faro, Portugal, September 1-5, 1996

QCD predictions are expected to give a better description of the data.

One particular problem at LEP 1.5 is that the majority of events is radiative (Fig. 1). Frequently the incoming electron or positron emits an energetic photon (usually at low polar angles) leading to an effective center-of-mass energy close to the  $Z$  mass. These radiative returns to the  $Z$  are characterized by two acollinear jets with an energetic photon, either detected in the forward calorimeters or escaped along the beam pipe.

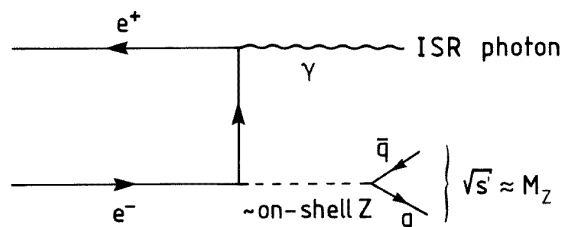


Figure 1: Illustration of radiative returns to the  $Z$  in  $e^+e^-$  interactions at a center-of-mass energy larger than  $M_Z$ .

The goal, of course, here is to study multiparticle dynamics at  $\sqrt{s} = 130-140$  GeV, and not to investigate the decay of almost real  $Z$ 's.

To select a sample of hadronic events at the full center-of-mass energy one can tag initial state radiation photons with the luminosity calorimeters or use the event kinematics to reject radiative events. The separation between radiative and non-radiative events is essential.

For physics comparisons the data taken at 130 GeV and 136 GeV are energy corrected to  $\sqrt{s} = 133$  GeV and averaged. Table 1 shows the number of hadronic events obtained by the four LEP detectors.

ALEPH	DELPHI	L3	OPAL
299	346	402	291

Table 1: Number of hadronic events at  $\sqrt{s} = 133$  GeV<sup>1;2;3;4</sup>.

The different event numbers are largely due to different cuts against radiative events.

## 2. Hadron Production

Hadron production in  $e^+e^-$  interactions proceeds in four steps<sup>5</sup>:

1. The electroweak theory describes the production of a gauge boson ( $Z$  or  $\gamma$ ) in  $e^+e^-$  collisions.

2. The gauge boson produces a quark-antiquark pair which initiates a quark-gluon cascade. As long as the energies of the partons are sufficiently high this cascade can be described by perturbative QCD.
3. The transformation of coloured partons to colour-neutral hadrons ("hadronization") cannot be calculated by quantum chromodynamics but requires Monte Carlo models which have been tuned to fit the data at  $\sqrt{s} = 91 \text{ GeV}$ .
4. Finally the end products of the hadronization process (primary hadrons, colour-neutral clusters or "clans") decay into the observed final state hadrons. Only longlived hadrons (lifetime  $> 1 \text{ ns}$ ) are directly seen in the detectors.

When the data are compared to QCD predictions various hadronization models are used. The JETSET event generator is based on the string fragmentation model. It exists in a matrix element (up to order  $\alpha_s^2$ ) and a parton shower version. It has been recently integrated into PYTHIA, which describes in addition to  $e^+e^-$ -interactions also hard ep and pp scattering. For  $e^+e^-$ -annihilation JETSET PS and PHYTIA are equivalent. HERWIG is based on the cluster fragmentation model, while ARIADNE uses radiation from colour dipoles with string fragmentation. COJETS incorporates independent fragmentation.

### 3. Particle Identification

Particle identification in the four LEP detectors relies on the multiple measurement of the specific energy loss  $dE/dx$  and/or the determination of Cherenkov-ring radii in RICH counters. Fig. 2 shows the  $dE/dx$  and RICH-information for a set simulated and Fig. 3 for observed events<sup>6</sup>. Clearly, a  $K-p$  separation can be obtained in certain kinematic ranges. The characteristic shower profiles in electromagnetic and hadronic calorimeters can be used to distinguish electrons from hadrons, and the penetration through hadron calorimeters identifies muons. For shortlived particles (100 fs  $> 1 \text{ ns}$ ) secondary vertices can be reconstructed and very shortlived particles are identified by the invariant mass of their decay products.

### 4. Total Cross-Section and Global Event Properties

The total cross-section  $\sigma_{\text{tot}}(e^+e^- \rightarrow \text{hadrons})$  is well described by the Standard Model. The cross-section is dominated by a pronounced radiative tail. Fig. 4<sup>7</sup> shows the results of the L3 experiment with data points at 130, 136 and 140 GeV along with lower energy data. Also shown is the result of the ALEPH experiment<sup>8</sup> from the recent run at  $\sqrt{s} = 161 \text{ GeV}$ . If the data samples are restricted to final states with visible hadronic energies close to the respective center-of-mass energy also agreement with expectation is observed.

The global event shapes of hadronic final states can be characterized by topological

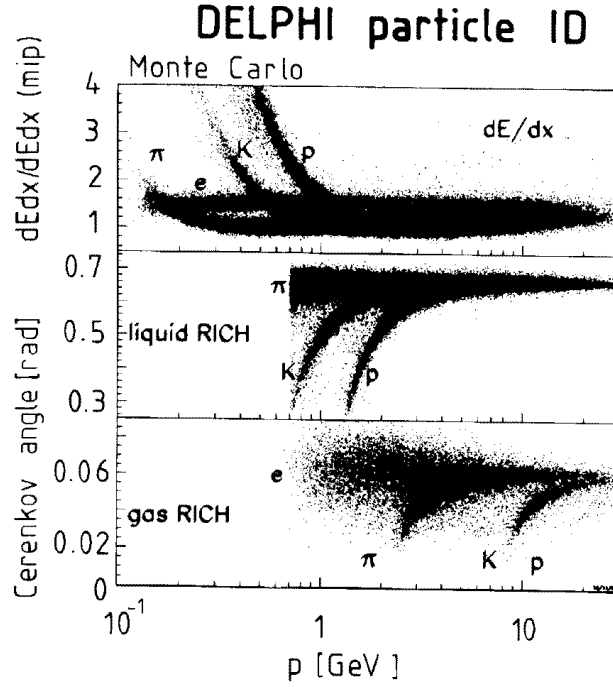


Figure 2:  $dE/dx$  and RICH information for simulated charged particles in multi-hadronic events <sup>6</sup>.

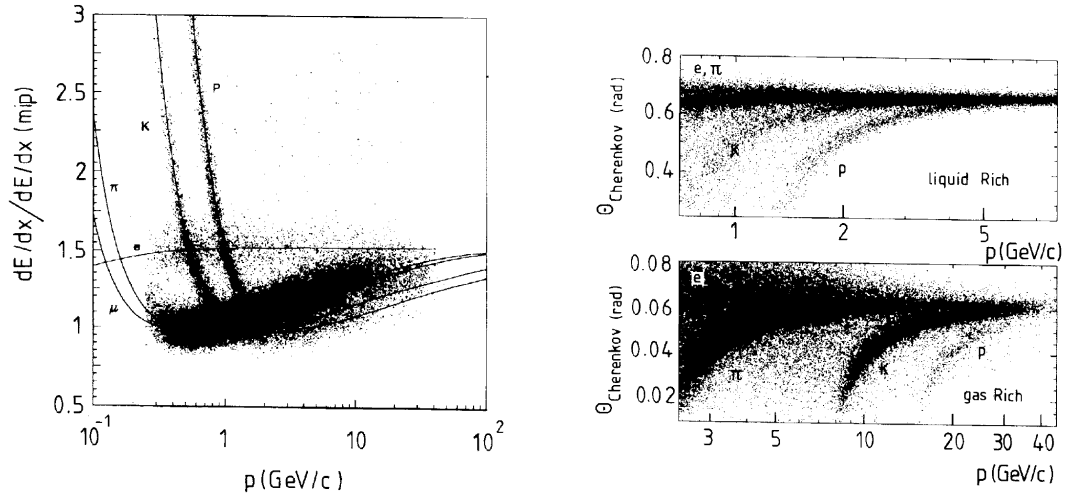


Figure 3:  $dE/dx$  and RICH information for reconstructed charged particles in multi-hadronic events <sup>6</sup>.

variables. The thrust-distributions (Fig.5) observed by ALEPH <sup>1</sup> and OPAL <sup>4</sup>, where

$$T = \max_{\vec{n}} \frac{\sum_i |\vec{p}_i \cdot \vec{n}|}{\sum_i |\vec{p}_i|}$$

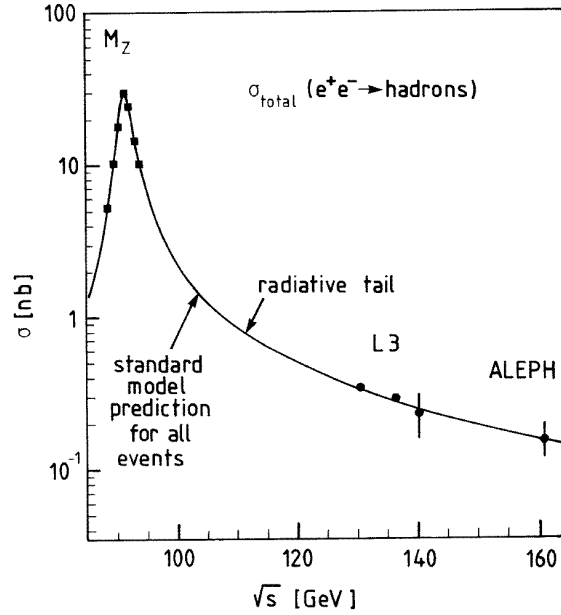


Figure 4: Cross-section for the process  $e^+e^- \rightarrow \text{hadrons}$ . The solid line is the Standard Model prediction for the total cross section <sup>7</sup>.

( $p_i$  are the momenta of the final state hadrons), show in general good agreement with Monte Carlo models, maybe with the exception of a small excess at low thrust values observed by ALEPH. Fig. 6 <sup>9</sup> shows as an example an event display of such a low

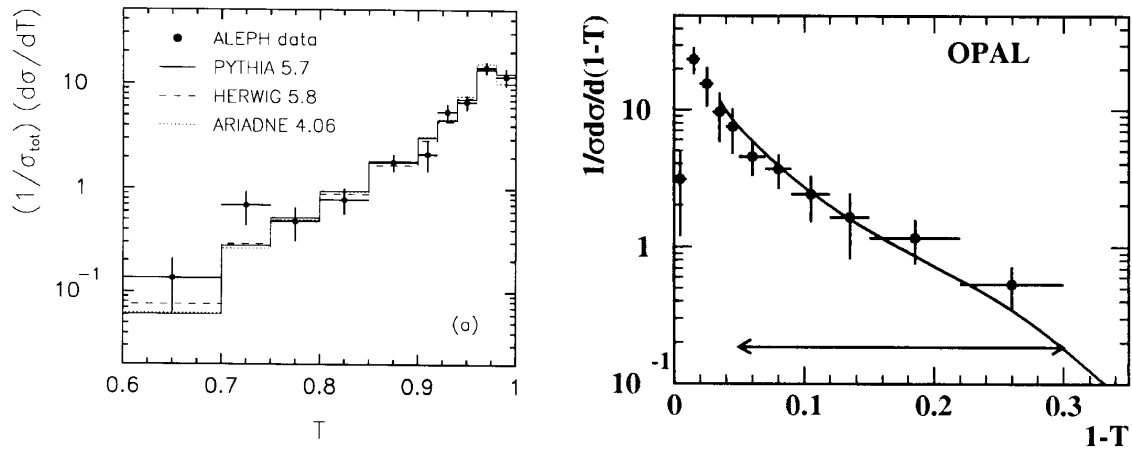


Figure 5: Thrust distribution at a center-of-mass energy of 133 GeV <sup>14</sup>.

thrust, near spherical event. The energy evolution of  $hT$  is well described by the models.

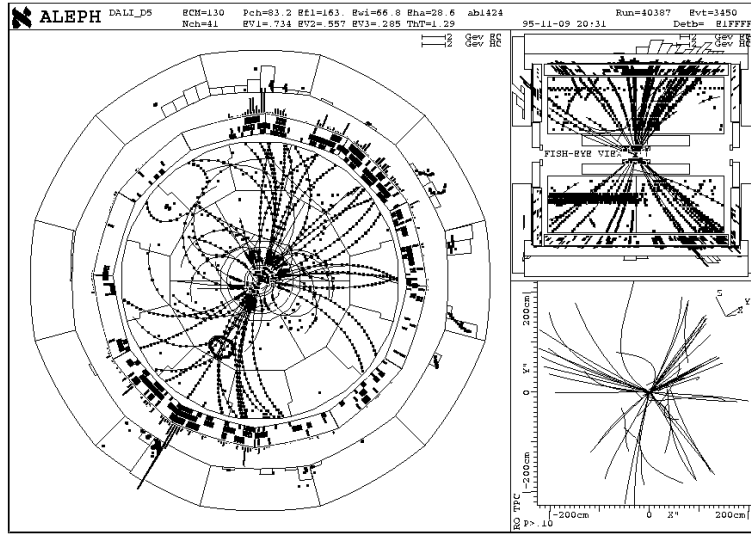


Figure 6: ALEPH event display of a low thrust, high multiplicity event <sup>9</sup>.

The distributions in rapidity

$$y = \frac{1}{2} \ln \frac{E + p_k}{E - p_k} ; \quad p_k = p_{\text{thrust}}$$

from ALEPH <sup>1</sup> and OPAL <sup>4</sup> also show agreement with models (Fig. 7 <sup>1/4</sup>). The small excess seen by ALEPH at low rapidities is related to the excess of low thrust events. The OPAL data clearly indicate that the COJETS Monte Carlo model with independent fragmentation fails to describe the data at low rapidities.

The sphericity tensor allows to investigate the planarity of events. It is given by

$$S = \frac{\sum_i p_i p_i}{\sum_i p_i^2} ; \quad i = 1; 2; 3$$

where  $p_i$  are the final state particle momenta with their components  $i = 1; 2; 3$ . This momentum tensor permits to define the transverse momentum in the event plane  $p_T^{\text{in}}$  with respect to the major sphericity axis and also the transverse momentum out of the event plane  $p_T^{\text{out}}$ . Within the statistics agreement between observation and model predictions is observed (Fig. 8 <sup>1/4</sup>). The disagreement between experimental data and models observed at  $\sqrt{s} = 91 \text{ GeV}$  in the  $p_T^{\text{out}}$  distribution at large  $p_T^{\text{out}}$  [e.g. <sup>10</sup>] is not confirmed at  $\sqrt{s} = 133 \text{ GeV}$ . Agreement is also observed at the recent high energy run at  $\sqrt{s} = 161 \text{ GeV}$ , albeit at low statistics.

The comparison of jet rates with prediction requires a jet counting algorithm. Jets are normally defined by the Durham clustering scheme. The quantity

$$Y_{ij} = 2 \frac{\min(E_i^2, E_j^2) (1 - \cos \theta_{ij})}{E_{\text{vis}}^2}$$

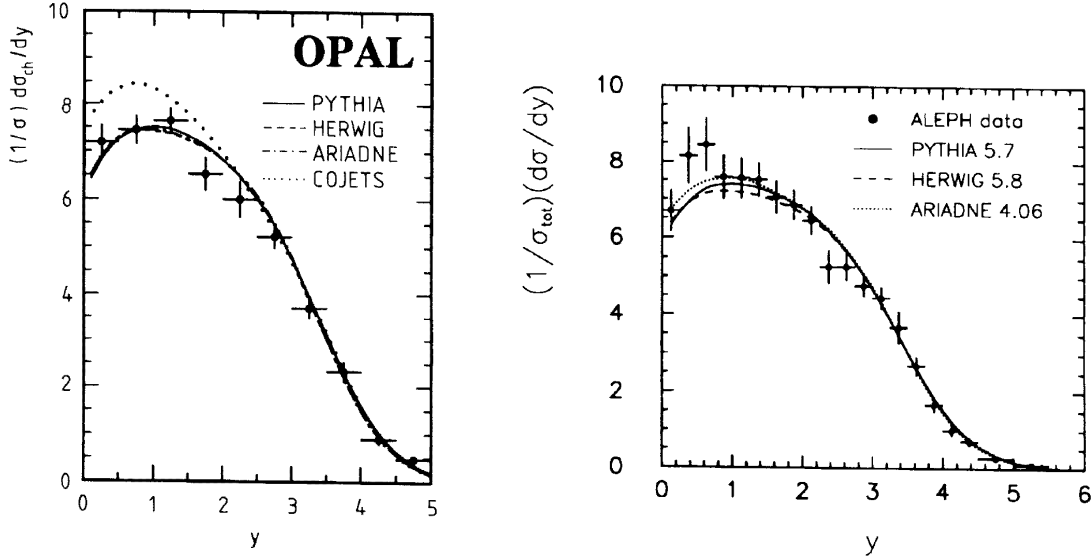


Figure 7: Rapidity distribution from ALEPH<sup>1</sup> and OPAL<sup>4</sup>.

with  $E_i, E_j$  - particle energies and  $\theta_{ij}$  - opening angle between the two particles, is calculated for all two-particle combinations. The pair with the smallest  $y_{ij}$  is replaced by a pseudoparticle by adding the four momenta of the two particles. For a given  $y$ -value  $y_{cut}$  the number of pseudoparticles gives the number of jets  $N_J$ . If  $y$  is extremely small  $N_J$  is equal to the multiplicity of charged particles in the event.  $y_{cut} = 0.1$  selects symmetric three-jet events, and for even larger values the particles are clustered into two jets. Instead of the Durham clustering scheme, also the JADE-algorithm can be used by defining

$$y_{ij} = \frac{2E_i E_j (1 - \cos \theta_{ij})}{E_{vis}^2}$$

with an analogous iteration procedure.

The ALEPH results on jet rates as a function of the jet resolution parameter  $y_{cut}$  displayed in Fig. 9<sup>1</sup> show in general good agreement with model predictions, although JETSET O( $s^2$ ) fails to reproduce the 5-jet rate. This is not a surprise because the matrix element version of JETSET O( $s^2$ ), which is only up to second order in  $s$ , can produce only four partons ( $e^+e^- \rightarrow qqg$  or  $e^+e^- \rightarrow qq\bar{q}q$ ).

The  $s$ -values derived from the global event properties of the four LEP experiments show agreement among each other leading to a LEP average of

$$s = 0.110 \pm 0.006 \quad \text{at} \quad \sqrt{s} = 133 \text{ GeV} :$$

Compared to the LEP I value of<sup>11</sup>

$$s = 0.118 \pm 0.005$$

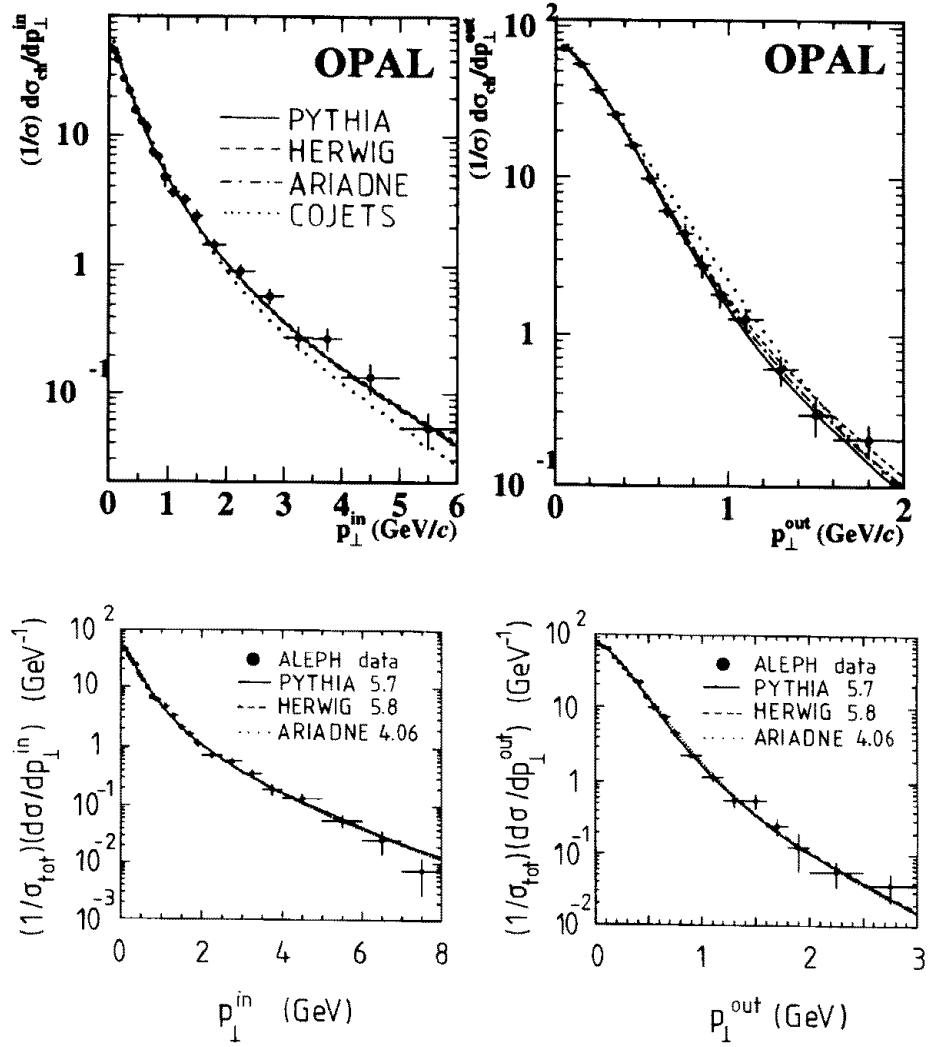


Figure 8: Transverse momentum distribution  $p_{\perp}^{\text{in}}$  and  $p_{\perp}^{\text{out}}$  from ALEPH<sup>1</sup> and OPAL<sup>4</sup>.

the LEP 1.5 result is lower by about one standard deviation, confirming the running of the strong coupling constant.

## 5. Multiplicities

The amount of data is sufficient to determine average charged multiplicities at 130 and 136 GeV separately. To study multiplicity distributions in detail requires more data so that at the moment no firm conclusion can be drawn on whether KNO-scaling is valid or whether the distributions are best reproduced by a log-normal or negative binomial distribution.



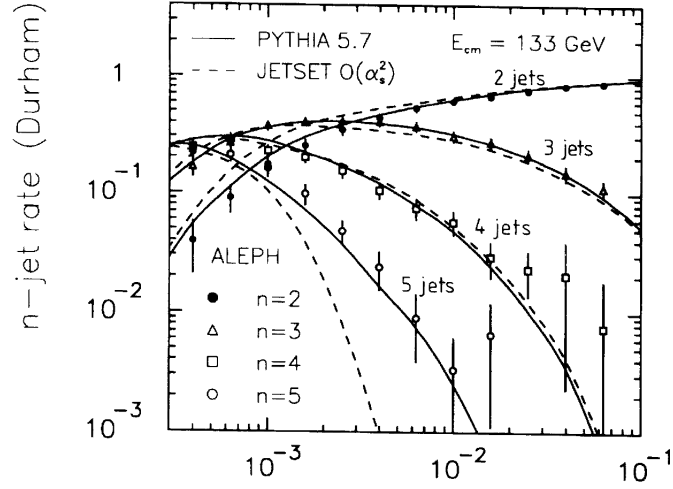


Figure 9:  $n$ -jet rates in their dependence on the  $y_{\text{cut}}$  value from ALEPH<sup>1</sup> at 133 GeV.

The results of the four LEP experiments on the average charged multiplicity in comparison to model predictions are shown in Table 2<sup>1;2;3;4</sup>. Fig. 10 shows L3 data in comparison to results at lower center-of-mass energies<sup>3</sup>. Also the average charged multiplicity from the recent run at 161 GeV obtained by ALEPH,  $\langle n_{\text{ch}} \rangle_{161 \text{ GeV}} = 25.8 \pm 1.0$  is shown in the figure.

	130 GeV	133 GeV	136 GeV
ALEPH	23.61 ± 0.65	24.15 ± 0.55	25.01 ± 0.79
DELPHI	23.84 ± 0.73		
L3	24.9 ± 0.9		24.2 ± 1.1
OPAL		23.40 ± 0.65	
JETSET PS		24.2	
HERWIG		24.1	
ARIADNE		24.1	
JETSET O <sub>s</sub> <sup>2</sup>		22.6	

Table 2: LEP results on the average charged multiplicity  $\langle n_{\text{ch}} \rangle$  in comparison with model predictions<sup>1;2;3;4</sup>.

The experimentally observed energy evolution of the charged particle multiplicity practically rules out the matrix element version of JETSET O<sub>s</sub><sup>2</sup> and the COJETSM model with independent fragmentation. JETSET PS and HERWIG describe the data

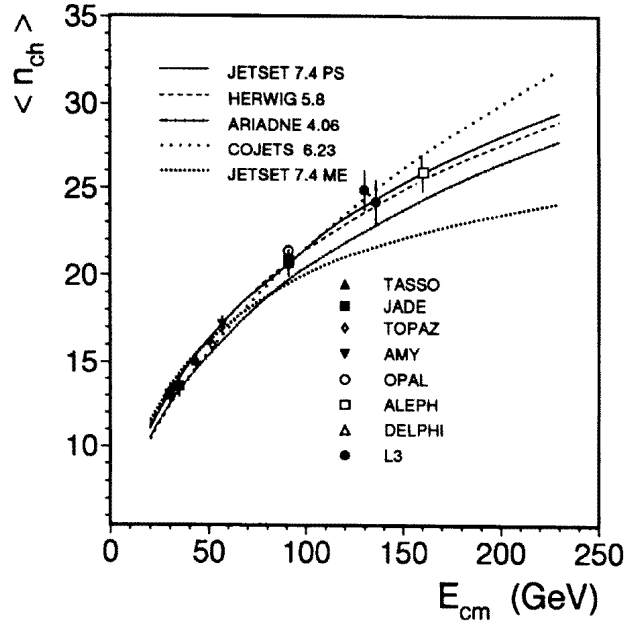


Figure 10: Average charged multiplicity as a function of the center-of-mass energy<sup>3</sup>.

rather well, while ARIADNE predicts somewhat low values.

## 6. Inclusive Particle Production

The small amount of data does not allow a meaningful determination of inclusive particle production rates for pions, kaons and protons separately. Fig. 11<sup>1</sup> shows the all particle momentum distribution in terms of the variable  $y = \ln 1/x_p$ , where  $x_p = p_{hadron}/p_{beam}$ . The variable  $y$  emphasizes the low momentum region (large values). Good agreement is observed with the Monte Carlo models. Also the energy evolution of the maximum of the  $y$ -distribution ( $y_{max}$ ) is well described by a modified leading-log approximation (MLLA)<sup>4</sup>.

## 7. Four Jet Events

In a search for  $e^+e^- \rightarrow X_1 X_2 \rightarrow$  four jets, where  $X_1$  and  $X_2$  are heavy particles decaying into two jets each, ALEPH has found a few events with interesting features. If the hadronic final states are clustered into four jets, if a rescaling of the jet energies using the well measured jet directions is made, and if QCD events are suppressed by a cut on the di-jet masses, a clustering of nine events in the sum of di-jet masses at 105 GeV is observed where the pairing is made by grouping two jets together which lead to the smallest di-jet mass difference<sup>12</sup>. The expected QCD background in the 63 GeV wide mass window centered on the 105 GeV mass peak is low ( $< 1$  event). An

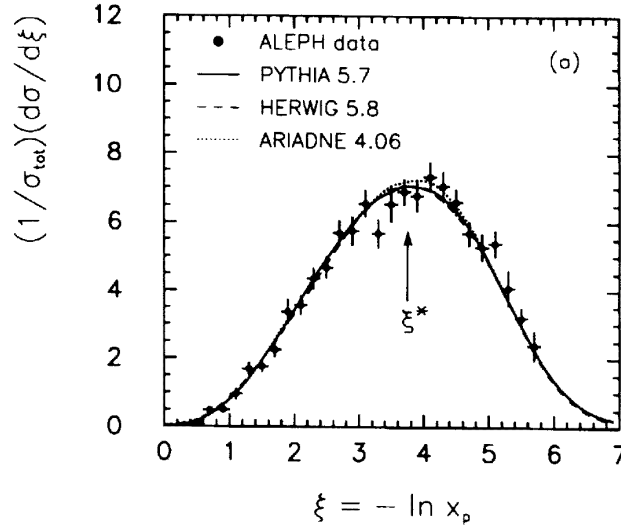


Figure 11: Allparticle distribution at 133 GeV observed by ALEPH .

analysis of the other three LEP-collaborations does not confirm the ALEPH finding, although DELPHI, L3 and OPAL in a similar analysis also find somewhat more events than predicted, but without any sign of clustering at a particular mass<sup>13</sup>. The few anomalous ALEPH events are also responsible for them in excess observed in the low thrust and low rapidity region (Fig. 5 and 7). The full analysis of the measurements at  $\sqrt{s} = 161$  GeV taken in July/August 1996 and the high energy run at the end of this year (presumably at  $\sqrt{s} = 172$  GeV) will probably settle the question whether the ALEPH excess is real or just a statistical fluctuation.

#### 8. Running at a center-of-mass energy of 161 GeV

The LEP experiments have collected about  $11 \text{ pb}^{-1}$  each at  $\sqrt{s} = 161$  GeV in a run in July/August 1996. All experiments have seen  $W^+W^-$  pair events (30 events per experiment) in the expected final states ( $qqqq$ ;  $qq\ell\ell$ ;  $\ell\ell\ell\ell$ ) with the predicted cross-sections.

A preliminary analysis of the QCD events shows good agreement with expectations.

#### 9. Conclusions

The analysis of the data taken at  $\sqrt{s} = 133$  GeV shows good agreement for the average charged multiplicity, the maximum value of the  $\xi$ -distribution,  $\xi^*$ , and the strong coupling constant in comparison to expectations from QCD. The global event properties are well described by JETSET PS, HERWIG and ARIADNE Monte Carlo models, while COJETS (with independent fragmentation) and JETSET O ( $\alpha_s^2$ ) are

less successful. ALEPH has found a small sample of potentially interesting four-jet events. The evidence, however, is not supported by DELPHI, L3 and OPAL, and also not by a first look at the data taken at  $\sqrt{s} = 161 \text{ GeV}$ .

## 10. Acknowledgements

The author is grateful to the conference organizers for the hospitality and the pleasant atmosphere at the symposium. I also thank Claudia Hauke and Volker Schreiber for their help in preparing the written version of my talk.

## 11. References

1. ALEPH-Collaboration D. Buskulic et al. CERN-PPE/96-43 (1996)
2. DELPHI-Collaboration P. Abreu et al. CERN-PPE/96-05 (1996)  
and Phys. Lett B 372 (1996) 172
3. L3-Collaboration M. Acciarri et al. CERN-PPE/95-192 (1995)  
and Phys. Lett B 371 (1996) 137
4. OPAL-Collaboration G. Alexander et al. CERN-PPE/96-47 (1996)
5. C. Grupen Proc. XXV Int. Sym p. on Multiparticle Dynamics 1995  
Stara Lesna; ed. D. Bruncko, L. Sandor, J. Urban p. 395, and references  
therein
6. DELPHI-Collaboration P. Abreu et al. CERN-PPE/95-194 (1995)
7. L3-Collaboration M. Acciarri et al. CERN-PPE/95-191 (1995)
8. ALEPH-Collaboration D. Buskulic et al. Contribution to the Int. Conf. on  
High Energy Physics, Warsaw 1996
9. ALEPH-Collaboration D. Buskulic et al. DALI-Program, H. Drevmann  
(1995)
10. G. Rudolph, these proceedings
11. M. Schmelling Phys. Scripta 51 (1995) 683
12. ALEPH-Collaboration D. Buskulic et al. CERN-PPE/96-52 (1996)  
and Z. Phys. C 71 (1996) 179
13. G. Rolandi, ALEPH-Physics Note 96-20 (1996)